

Building quantum neural networks based on swap test

Jian Zhao,^{1,2} Yuan-Hang Zhang,³ Chang-Peng Shao,^{4,*}
Yu-Chun Wu,^{1,2,†} Guang-Can Guo,^{1,2} and Guo-Ping Guo^{1,2,5,‡}

¹Key Laboratory of Quantum Information, Chinese Academy of Sciences, School of Physics,
University of Science and Technology of China, Hefei, Anhui, 230026, P. R. China

²CAS Center For Excellence in Quantum Information and Quantum Physics,
University of Science and Technology of China, Hefei, Anhui, 230026, P. R. China

³School of the Gifted Young, University of Science and Technology of China, Hefei, Anhui, 230026, P.R. China.

⁴Academy of Mathematics and Systems Science, Chinese Academy of Sciences, Beijing 100190, China

⁵Origin Quantum Computing Hefei, Anhui 230026, P. R. China

Artificial neural network, consisting of many neurons in different layers, is an important method to simulate human brain. Usually, one neuron has two operations: one is linear, the other is nonlinear. The linear operation is inner product and the nonlinear operation is represented by an activation function. In this work, we introduce a kind of quantum neuron whose inputs and outputs are quantum states. The inner product and activation operator of the quantum neurons can be realized by quantum circuits. Based on the quantum neuron, we propose a model of quantum neural network in which the weights between neurons are all quantum states. We also construct a quantum circuit to realize this quantum neural network model. A learning algorithm is proposed meanwhile. We show the validity of learning algorithm theoretically and demonstrate the potential of the quantum neural network numerically.

PACS numbers: 03.65.Ud, 03.67.Mn

I. INTRODUCTION

Artificial neural networks can be traced back to McCulloch-Pitts (M-P) neurons proposed in 1943 [1]. Based on M-P neurons, Rosenblatt in 1957 proposed the perceptron model with a learning algorithm [2]. So far, artificial neural networks have had certain theoretical bases [3, 4] and extensive practical applications ranging from modeling, classification, pattern recognition to multivariate data analysis [5, 6].

Quantum neural networks, proposed by Kak [7] first in 1995, is a class of neural networks that combine quantum information theory and artificial neural networks. Different models related to quantum neural networks have been developed [8–16]. Among these models, Ref. [9] is a perceptron model with quantum input, quantum output, and weights represented by operators, in which the concrete construction is not explained; Ref. [15] uses quantum computing to achieve the potential acceleration of classical neural networks; Ref. [16] is based on the actual physical device to construct an analog classical neural network. However, there is still no uniform standard for the rigorous definition of quantum neural networks.

Recently, the paper [17] introduced a strategy for using quantum phase estimation to get the information for the inner product of two quantum states. Inspired by this work, we introduce a definition of quantum neuron with quantum states as input states, weights and a single-particle state as the output state. Accordingly we pro-

pose a quantum neural network which can be represented by quantum circuits. Besides, through theoretical analysis and the numerical experiment we demonstrate the validity of the learning algorithm.

Our starting point is to assume that there is a large amount of quantum states, each of which is labeled by a quantum state. Given these data as the training set, our goal is to predict the label of an unknown input state. It is convenient for our proposed quantum neurons to process quantum data directly. And it does not cost the classical computing resources to perform the trained quantum neural networks. If using classical neural networks, one may need the method of quantum-state tomography to reconstruct the quantum data [18], which is a highly complex task itself.

This proposed neuron adapts to different kinds of data flexibly. When quantum states as the quantum data are labeled by real numbers rather than quantum states, we can slightly modify the measured strategy to realize classical outputs. Things get more complicated when both data and labels are classical. If using this proposed neuron we need to consider the state preparation problem, which requires controlling the amplitude of the desired quantum state to realize effectiveness [19, 20]. A method making state preparation simple is to limit the structure of the data [21], in which they limit data to the vectors with binary value components.

The paper is organized as follows. At the end of this section we briefly state the notations used in this paper. In section II, we describe the swap test and its quantum circuit. In section III, we construct a quantum neuron according to our proposed definition, and then we analyze the property of this proposed quantum neuron. The proof process is put in Appendix A. In section IV, based

* Email address: cphshao@amss.ac.cn

† Email address: wuyuchun@ustc.edu.cn

‡ Email address: gpguo@ustc.edu.cn

on the construction of quantum neuron we construct a kind of feedforward neural network and a quantum circuit model representing the specific quantum neural network. We give quantitative estimations of success probability and fidelity theoretically. Some details are presented in Appendix B. We put the training process of the quantum neural network in section V. And in section VI we present an experiment for numerical simulation. At last in section VII, we draw the conclusions of this paper.

Notation. We use capital Roman letters A, B, \dots , for matrices, lower case Roman letters x, y, \dots , for column vectors, and Greek letters α, β, \dots , for scalars. For a scalar α , we denote by $\mathbf{Re}\alpha$ and $\mathbf{Im}\alpha$ the real and imaginary part of α , respectively. Given a column vector x , x^T denotes its transpose and $x^\dagger \triangleq (\bar{x})^T$ is its conjugate transpose, and similar for a given matrix A . Specifically, for the unitary transformation U , $U^\dagger = U^{-1}$. A quantum state $|x\rangle \in \mathbb{C}^{2^n}$ is regarded as the normalized vector. We write $R_Y(\beta) = \begin{bmatrix} \cos \frac{\beta}{2} & -\sin \frac{\beta}{2} \\ \sin \frac{\beta}{2} & \cos \frac{\beta}{2} \end{bmatrix}$ and $R_Z(\gamma) = \begin{bmatrix} e^{-i\frac{\gamma}{2}} & 0 \\ 0 & e^{i\frac{\gamma}{2}} \end{bmatrix}$.

II. SWAP TEST AND ITS QUANTUM CIRCUIT

The swap test method has been applied widely to quantum machine learning [22–24]. In this section, we describe the swap test and its quantum circuit.

Let $|x\rangle, |w\rangle \in \mathbb{C}^{2^n}$ be two quantum states that are prepared by unitary operators U_x, U_w respectively. That is $|x\rangle = U_x|0\rangle^{\otimes n}, |w\rangle = U_w|0\rangle^{\otimes n}$. Swap test is a technique that can be used to estimate $\langle x|w\rangle$. The basic procedure can be stated as follows:

Step 1. Prepare the state

$$|\phi_r\rangle = \frac{1}{\sqrt{2}}(|+\rangle|x\rangle + |-\rangle|w\rangle). \quad (1)$$

The quantum circuit to prepare $|\phi_r\rangle$ is simple; see Figure 1 below. We denote the unitary to prepare $|\phi_r\rangle$ as U_{ϕ_r} .

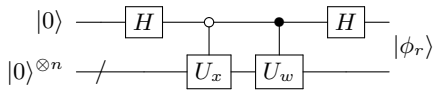


FIG. 1. Quantum circuit to prepare $|\phi_r\rangle$

Step 2. Construct the unitary transformation

$$\begin{aligned} G_r &= (I^{\otimes(n+1)} - 2|\phi_r\rangle\langle\phi_r|)(Z \otimes I^{\otimes n}) \\ &= U_{\phi_r}(I^{\otimes(n+1)} - 2|0\rangle^{\otimes(n+1)}\langle 0|^{\otimes(n+1)})U_{\phi_r}^\dagger(Z \otimes I^{\otimes n}), \end{aligned} \quad (2)$$

where $Z = |0\rangle\langle 0| - |1\rangle\langle 1|$ is the Pauli-Z matrix. The circuit to implement G_r is represented in Figure 2. As for the unitary operator $I^{\otimes(n+1)} - 2|0\rangle^{\otimes(n+1)}\langle 0|^{\otimes(n+1)}$, we can run it in the circuit shown in Figure 3.

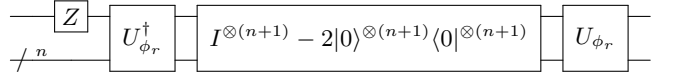


FIG. 2. Quantum circuit to implement G_r

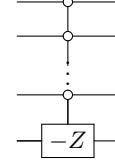


FIG. 3. Quantum circuit to run $I^{\otimes(n+1)} - 2|0\rangle^{\otimes(n+1)}\langle 0|^{\otimes(n+1)}$

The state $|\phi_r\rangle$ can be rewritten as

$$|\phi_r\rangle = \frac{1}{2}(|0\rangle(|x\rangle + |w\rangle) + |1\rangle(|x\rangle - |w\rangle)). \quad (3)$$

The amplitude of $|0\rangle$ is $\sqrt{1 + \mathbf{Re}\langle x|w\rangle}/\sqrt{2}$, and the amplitude of $|1\rangle$ is $\sqrt{1 - \mathbf{Re}\langle x|w\rangle}/\sqrt{2}$. Denote $|u\rangle$ and $|v\rangle$ as the normalized states of $|x\rangle + |w\rangle$ and $|x\rangle - |w\rangle$ respectively. Then there is a real number $\theta_r \in [0, \pi/2]$ such that

$$|\phi_r\rangle = \sin\theta_r|0\rangle|u\rangle + \cos\theta_r|1\rangle|v\rangle. \quad (4)$$

Moreover, θ_r satisfies $\cos\theta_r = \sqrt{1 - \mathbf{Re}\langle x|w\rangle}/\sqrt{2}$, i.e.,

$$\mathbf{Re}\langle x|w\rangle = -\cos 2\theta_r. \quad (5)$$

Apply the Schmidt decomposition method to the quantum state $|\phi_r\rangle$, and we can decompose it into

$$|\phi_r\rangle = \frac{-i}{\sqrt{2}}(e^{i\theta_r}|w_+\rangle - e^{-i\theta_r}|w_-\rangle), \quad (6)$$

where $|w_\pm\rangle = \frac{1}{\sqrt{2}}(|0\rangle|u\rangle \pm i|1\rangle|v\rangle)$. Besides, it is easy to check that

$$G_r|w_\pm\rangle = e^{\pm i2\theta_r}|w_\pm\rangle. \quad (7)$$

This means $|w_\pm\rangle$ are the eigenstates of G_r . The information of θ is contained in the arguments of the eigenvalues.

Step 3. Use quantum phase estimation algorithm to estimate θ . The quantum circuit is shown in Figure 4.

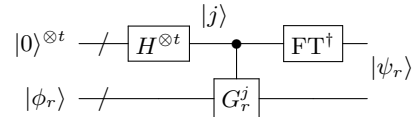


FIG. 4. Quantum phase estimation to estimate θ

In Figure 4, t is an integer relates to the precision, and FT is the quantum Fourier transform. The control gate G_r^j should be regarded as a composition of a series of controlled gates $G_r^{2^i}$ by viewing the i -th qubit in the first register as control qubit, where $i = 0, \dots, t-1$.

By equations (6) and (7), the output of quantum phase estimation is an approximate of

$$|\psi_r\rangle = \frac{-i}{\sqrt{2}}(e^{i\theta_r}|y_r\rangle|w_+\rangle - e^{-i\theta_r}|2^t - y_r\rangle|w_-\rangle), \quad (8)$$

where $y_r \in [0, 2^{t-1}]$ and $y_r\pi/2^{t-1}$ is an approximate of $2\theta_r$. By equation (5), we have

$$\mathbf{Re}\langle x|w\rangle \approx -\cos(\pi y_r/2^{t-1}). \quad (9)$$

Note that $\mathbf{Im}\langle x|w\rangle = -\mathbf{Re}\langle x|i|w\rangle$, thus the proposal to estimate the real part of inner product is also suitable to estimate $\mathbf{Im}\langle x|w\rangle$. We only need to consider the state $|\phi_i\rangle = \frac{1}{\sqrt{2}}(|+\rangle|x\rangle - |-\rangle|w\rangle)$. Finally, we will obtain a $y_i \in [0, 2^{t-1}]$, such that

$$\mathbf{Im}\langle x|w\rangle \approx -\cos(\pi y_i/2^{t-1}). \quad (10)$$

For convenience, the corresponding parameters, unitaries and quantum states used to estimate $\mathbf{Im}\langle x|w\rangle$ will be accordingly denoted by $\theta_i, y_i, U_{\phi_i}, G_i, U_{\psi_i}$ and $|\phi_i\rangle, |\psi_i\rangle$.

III. CONSTRUCTION OF THE QUANTUM NEURON

A. Definition of the quantum neuron

A classical neuron can be treated as a function that maps a vector $x = (x_1, \dots, x_n)^T \in \mathbb{R}^n$ to a real value $z = f(x^T w)$, where $w = (w_1, \dots, w_n)^T \in \mathbb{R}^n$ and f is usually a nonlinear function. $\{x_i\}_{i=1}^n$ and $\{w_i\}_{i=1}^n$ are called the input values and synaptic weights, respectively. The function f is called the activation function. Similarly, we propose the definition of quantum neuron as follows

Definition 1. Let $|w\rangle = |w_1, \dots, w_n\rangle \in (\mathbb{C}^2)^{\otimes n}$ be a product state. Denote $\mathcal{B}(0, 1) = \{a \in \mathbb{C} : |a| \leq 1\}$. Assume that f is a map from $\mathcal{B}(0, 1)$ to the subspace of \mathbb{C}^2 with unit norm, then the map

$$\begin{aligned} F : \mathbb{C}^{2^n} &\longrightarrow \mathbb{C}^2 \\ |x\rangle &\longmapsto f(\langle x|w\rangle) \end{aligned} \quad (11)$$

is called an n -variable quantum neuron.

In the n -variable quantum neuron, we call $|x\rangle$ the input state, $\{|w_i\rangle\}_i$ the (synaptic) weight states and $f(\langle x|w\rangle)$ the output state. The map f plays the role of activation function in defining the quantum neuron Figure 5 shows the basic structure of quantum neuron.

Assume that $a \in \mathbb{C}$, a commonly used activation function in this paper is

$$\begin{aligned} f(a) &= R_Z(-\frac{\pi}{2})R_Z(\arccos -\mathbf{Im}a)R_Y(\arccos -\mathbf{Re}a)|0\rangle \\ &= \begin{bmatrix} \cos(\frac{\arccos -\mathbf{Re}a}{2})e^{i(\frac{\pi}{4} - \frac{\arccos -\mathbf{Im}a}{2})} \\ \sin(\frac{\arccos -\mathbf{Re}a}{2})e^{-i(\frac{\pi}{4} - \frac{\arccos -\mathbf{Im}a}{2})} \end{bmatrix}. \end{aligned} \quad (12)$$

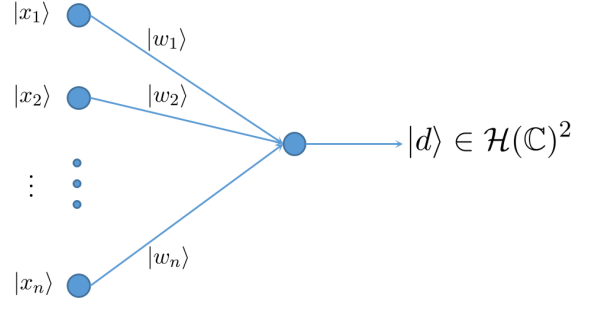


FIG. 5. Structure of quantum neuron, where $|d\rangle = f(\langle x|w\rangle)$ is the output state.

The operator $R_Z(-\pi/2)$ is added to make sure that if $a \in \mathbb{R}$, then

$$f(a) = \begin{bmatrix} \cos(\frac{\arccos -a}{2}) \\ \sin(\frac{\arccos -a}{2}) \end{bmatrix} \in \mathbb{R}^2.$$

B. Realization of the output state in the quantum circuit

Now assume that the activation function f is defined by equation (12). Let $|x\rangle \in \mathbb{C}^{2^n}$ be an input state and $|w\rangle \in (\mathbb{C}^2)^{\otimes n}$ be a weight state. In this subsection, we show how to realize $f(\langle x|w\rangle)$ in the quantum circuit.

We first show how to realize $f(\langle x|w\rangle)$ in the quantum circuit in the ideal case, then extend it into the general case. By ideal, we mean both $\frac{\arccos -\mathbf{Re}\langle x|w\rangle}{2\pi}$ and $\frac{\arccos -\mathbf{Im}\langle x|w\rangle}{2\pi}$ can be represented in binary form with t bits precisely. As a result, swap test can approximate these two values with no error, i.e., equations (9) and (10) are exact.

By equation (9), (10) and (12),

$$f(\langle x|w\rangle) = R_Z(-\pi/2)R_Z(\pi y_i/2^{t-1})R_Y(\pi y_r/2^{t-1})|0\rangle, \quad (13)$$

To prepare the state (13), first we consider $|\psi_r\rangle|0\rangle$, where $|\psi_r\rangle$ is given in equation (8). We want to generate the state $R_Y(\pi y_r/2^{t-1})|0\rangle$ in the third register of $|\psi_r\rangle|0\rangle$ by viewing $|y_r\rangle$ and $|2^t - y_r\rangle$ as control registers. That is to obtain the following transformation

$$\begin{aligned} |\psi_r\rangle|0\rangle &= \frac{-i}{\sqrt{2}}(e^{i\theta_r}|y_r\rangle|w_+\rangle - e^{-i\theta_r}|2^t - y_r\rangle|w_-\rangle)|0\rangle \\ &\mapsto |\psi_r\rangle R_Y(\pi y_r/2^{t-1})|0\rangle. \end{aligned}$$

The control rotation generated by $|y_r\rangle$ gives $R_Y(\pi y_r/2^{t-1})$ directly. However, the control rotation generated by $|2^t - y_r\rangle$ gives $R_Y(\pi(2^t - y_r)/2^{t-1}) = -XR_Y(\pi y_r/2^{t-1})X$. To modify this, it suffices to add a control X and control $-X$ gate. More precisely, assume that $y'_r \in \{y_r, 2^t - y_r\}$ and $y'_r = \sum_{j=0}^{t-1} 2^j y'_{r,t-j-1}$ in binary form, then the control qubit is $|y'_{r,0}\rangle$. If

$y'_{r,0} = 0$, then we know $y'_r = y_r$ and we just apply control rotation $R_Y(\pi y'_r/2^{t-1})$ to $|0\rangle$. If $y'_{r,0} = 1$, then we know $y'_r \in \{2^{t-1}, 2^t - y_r\}$. In this case, we apply X gate to $|0\rangle$ first, then apply control rotation $R_Y(\pi y'_r/2^{t-1})$, finally apply $-X$ to the result. The quantum circuit is shown in Figure 6(a).

If we consider $|\psi_i\rangle R_Y(\pi y_r/2^{t-1})|0\rangle$, then based on the fact $R_Z(\pi(2^t - y_i)/2^{t-1})|0\rangle = -X R_Z(\pi y_i/2^{t-1})X$ and the above analysis, we can generate $|\psi_i\rangle R_Z(\pi y_i/2^{t-1})R_Y(\pi y_r/2^{t-1})|0\rangle$ by the quantum circuit of Figure 6(b).

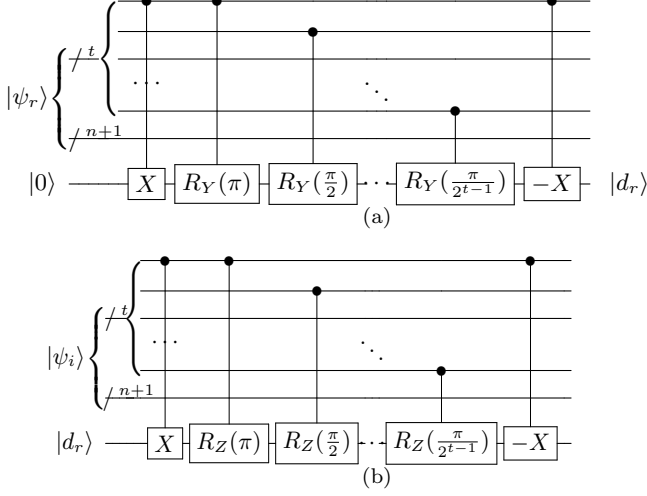


FIG. 6. The quantum neuron to generate $R_Z(\pi y_i/2^{t-1})|d_r\rangle$, where $|d_r\rangle = R_Y(\pi y_r/2^{t-1})|0\rangle$.

Finally, we conclude the above two procedures in Figure 7 by adding $R_Z(-\pi/2)$ to generate $f(\langle x|w\rangle)$, where $R_{Y_{f_r}}(t)$ and $R_{Z_{f_i}}(t)$ are short for the control operators used in Figure 6(a) and Figure 6(b) respectively.

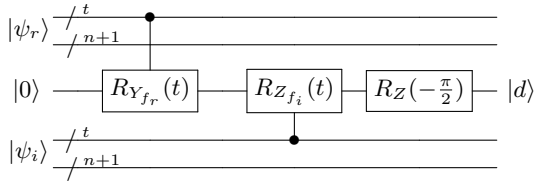


FIG. 7. The quantum neuron in the ideal case, where $|d\rangle = f(\langle x|w\rangle)$.

Generally, $\frac{\arccos -\text{Re}\langle x|w\rangle}{2\pi}$ and $\frac{\arccos -\text{Im}\langle x|w\rangle}{2\pi}$ cannot be written in binary form precisely. And y_r, y_i only give approximates of them. By introducing measurements to the original circuit, the quantum circuit given in Figure 8 returns an approximate of $f(\langle x|w\rangle)$ with high probability. For a detailed proof see Appendix A.

Theorem 1. Let $|x\rangle \in \mathbb{C}^{2^n}$ be a quantum state and $|w\rangle \in (\mathbb{C}^2)^{\otimes n}$ be a product state. Let $t = m + \lceil \log_2(2 + \frac{1}{\sigma}) \rceil$ be the number of ancilla qubits used in quantum phase estimation, where $\sigma \in (0, 1)$ and $m \in \mathbb{Z}^+$. Assume that $|\tilde{d}\rangle$ is the state obtained by the quantum

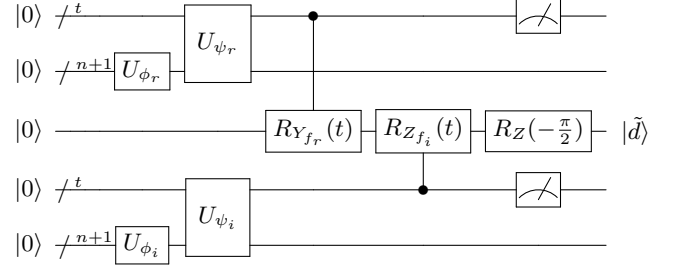


FIG. 8. The quantum neuron in the general case.

circuit given in Figure 8. Then with success probability at least $1 - \sigma$, we have $\| |\tilde{d}\rangle - |d\rangle \| \leq \pi/2^{m-1}$, where $|d\rangle = f(\langle x|w\rangle)$.

In Figure 8, the purpose of performing measurements is simply to convert the mixed state (A1) in the ancillary registers into a pure state $|\tilde{d}\rangle$ that is close to $f(\langle x|w\rangle)$. However, it is unnecessary to record or store the measured results, which makes it possible to perform quantum neurons without the classical resources.

One thing worth noting is that the quantum neuron model defined by Fig. 8 can be used to analyze quantum data with real number labels through analyzing the measured results $|\tilde{d}\rangle$. More precisely, assume that $|\tilde{d}\rangle = p_0|0\rangle + p_1|1\rangle$ is the output of Fig. 8. By equation (12), if we perform measurements to $|\tilde{d}\rangle$, then we can estimate

$$|p_1|^2 \approx \sin^2\left(\frac{\arccos -\text{Re}\langle x|w\rangle}{2}\right) = \frac{1 + \text{Re}\langle x|w\rangle}{2}.$$

The probability $|p_1|^2$ characterizes the closeness between $|\tilde{d}\rangle$ and $|1\rangle$. It can be viewed as the label of the input state $|x\rangle$. Note that to solve the classification problems by classical neural networks, we need to calculate a function of the inner product between the input and the weight. However, this inner product is already include in $|p_1|^2$. Thus classical classification problems can also be solved by quantum neuron. Especially for binary classification problems, we can simply define the label of $|x\rangle$ as a quantum state, e.g. $|0\rangle$ or $|1\rangle$.

IV. CONSTRUCTION OF THE QUANTUM NEURAL NETWORK

The classical feed-forward neural network has been used to process data to simulate unknown nonlinear functions [25–27]. In this section we introduce a quantum feed-forward neural network to accomplish a similar task.

Let $\mathcal{M} \triangleq \{|x^i\rangle : i = 1, \dots, q\} \subset \mathbb{C}^{2^n}$ be a quantum data set. We want to apply some kind of quantum feed-forward neural network to capture the property and structure of \mathcal{M} theoretically. More precisely, suppose that the information of \mathcal{M} is included in an unknown function F_0 mapping \mathcal{M} to a product state space with

dimensions 2^s , that is

$$F_0 : \quad M \longrightarrow (\mathbb{C}^2)^{\otimes s} \\ |x^i\rangle \longmapsto |d^i\rangle = |d_1^i, \dots, d_s^i\rangle. \quad (14)$$

Our purpose is to construct a neural network based on the quantum neuron to simulate F_0 efficiently.

Let $|x\rangle \in \mathcal{M}$ be the input state and it is allowed to be entangled. For convenience, we assume $|x\rangle$ a product state, that is $|x\rangle = |x_1, x_2, \dots, x_n\rangle$. The state $|x\rangle$ constitutes the input layer, i.e., the 0-th layer, of the quantum neural network. We denote it as $|z^{(0)}\rangle$. Suppose we have $K - 1$ hidden layers and one output layer. The output layer is also known as the K -th layer. Denote the number of neurons in the k -th layer as p_k , where $k = 1, \dots, K$ and $p_K = s$.

For $k = 1, \dots, K$, the j -th neuron in the k -th and $(k - 1)$ -th layers are connected by an edge with weight $|w_{ij}^{(k)}\rangle$, where $i = 1, \dots, p_{k-1}, j = 1, \dots, p_k$. The state of each neuron in the k -th layer is determined by the weights and the states of the $(k - 1)$ -th layer. Thus, if we denote by $|z_j^{(k)}\rangle$ as the state of the j -th neuron in the k -th layer, then

$$|z_j^{(k)}\rangle = f_j^{(k)}(\langle z^{(k-1)} | w_j^{(k)} \rangle), \quad (15)$$

where $|z^{(k-1)}\rangle = |z_1^{(k-1)}, \dots, z_{p_{k-1}}^{(k-1)}\rangle$, $|w_j^{(k)}\rangle = |w_{1j}^{(k)}, \dots, w_{p_{k-1}j}^{(k)}\rangle$, and $f_j^{(k)}$ is defined by equation (12). Figure 9 shows the basic structure of quantum neural network.

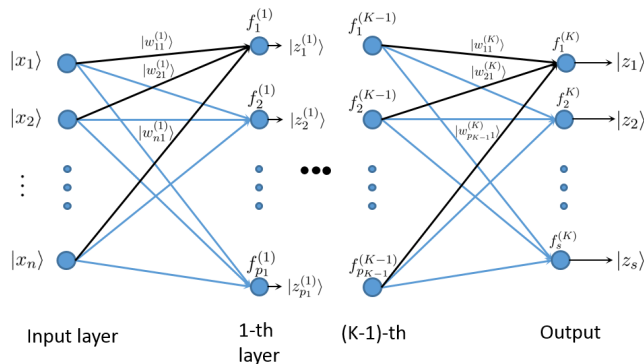


FIG. 9. The quantum feed-forward neural network

Example. We set $n = 2$, $p_1 = 2$, $K = 2$ and $p_2 = s = 1$. In this case the quantum neural network and the corresponding quantum circuit are shown in Figure 10 (a) and Figure 10 (b), respectively.

In the construction of circuits we use the strategy of postponing measurement. To be specific, we postpone the measured process of each neuron in all hidden layers until the last layer. In Figure 10 (b) we postpone $4t$ measured results in the first layer.

The strategy of postponing measurement is necessary. Suppose we want to get the output state of the neuron

in hidden layers, we need to measure the corresponding qubits to convert the mixed state to a random pure state. Without postponing measurement we cannot use the method of swap test to get the subsequent output states, which means the neural network is interrupted. This implies that the intermediate state is unreadable in the quantum neural network and we do not care about the state of hidden layer neurons naturally.

In this quantum neural network, we give quantitative estimations of success probability and fidelity for the output state. Its proof is presented in Appendix B.

Theorem 2. Given a quantum neural network defined in Figure 9. Suppose the number of the neurons in the k -th layer is p_k . Let $p = \max\{p_1, \dots, p_K\}$, $\epsilon \in (0, 1)$ and $\sigma \in (0, 1)$. Set $m = \lceil \log_2[(\frac{2\pi^2 p^2}{\epsilon})2^{K-1}\pi] \rceil + 1$ and $t = m + \lceil \log_2(2 + \frac{Kp}{\sigma}) \rceil$. Then with success probability at least $1 - \sigma$ we have the fidelity

$$\left\| |z^{(K)}\rangle - |\tilde{z}^{(K)}\rangle \right\| \leq \epsilon. \quad (16)$$

V. TRAINING PROCESS

In this section, we introduce the training process of the proposed quantum neural network. We transform the quantum neural network into a quantum circuit containing parameters to be optimized. The training process of parameterized quantum circuits has been used in many quantum algorithms [28–30].

Suppose the quantum neural network has n neurons in the input layer and has s neurons in the output layer. In training process, we choose the mean square loss

$$\begin{aligned} \mathcal{L}(\mathcal{M}, \mathcal{W}) &= \frac{1}{q} \sum_{i=1}^q \left| |z^i\rangle - |d^i\rangle \right|^2 \\ &= \frac{1}{q} \sum_{i=1}^q (2 - 2\text{Re}\langle z^i | d^i \rangle). \end{aligned} \quad (17)$$

Each input state $|x^i\rangle \in \mathcal{M}$ has a fixed label $|d^i\rangle = |d_1^i, \dots, d_s^i\rangle$. Each output state $|z^i\rangle = |z_1^i, \dots, z_s^i\rangle$ produced by quantum circuits can be closed to $|\tilde{z}^i\rangle$ with high success probability according to theorem 2, where $|\tilde{z}^i\rangle$ is the ideal output state decided by all the weights $|w_j^{(k)}\rangle$ and the activation function f defined in expression (12).

Our goal is to find a set $\mathcal{W} \triangleq \{|w_j^{(k)}\rangle : k = 1, \dots, K, j = 1, \dots, p_k\}$ of weight states such that they minimize the mean square loss.

Since $|w_j^{(k)}\rangle = |w_{1j}^{(k)}, \dots, w_{p_{k-1}j}^{(k)}\rangle$ is a product state, we assume that

$$|w_{ij}^{(k)}\rangle = e^{i\delta_{ijk}} R_Z(\gamma_{ijk}) R_Y(\beta_{ijk}) |0\rangle \quad (18)$$

for some parameters $\beta_{ijk}, \gamma_{ijk}, \delta_{ijk} \in [0, 2\pi)$ to be tuned. Denote the parameter vector by $\theta = (\theta_1, \dots, \theta_L)^T$, where

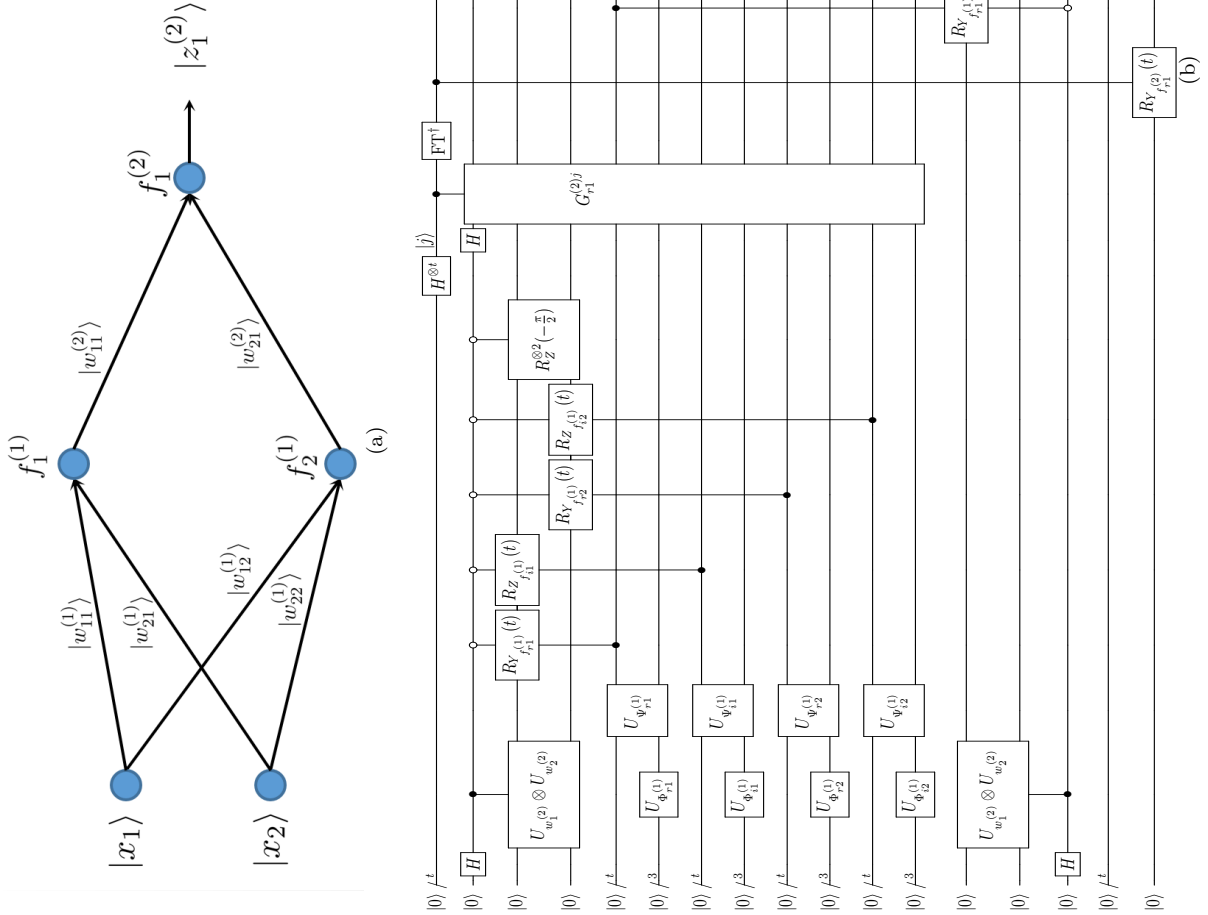


FIG. 10. **Construction of the quantum feedforward neural network.** Here the input states are $|x_1\rangle$ and $|x_2\rangle$, and the output state is $|z_1^{(2)}\rangle$. (a) **Quantum neural network model with 3 neurons.** (b) **The quantum neural network represented by a circuit.** The transformations $G_{r_1^{(2)}}$ and $G_{i_1^{(2)}}$ are controlled by 4t qubits compared to before; see Figure 11.

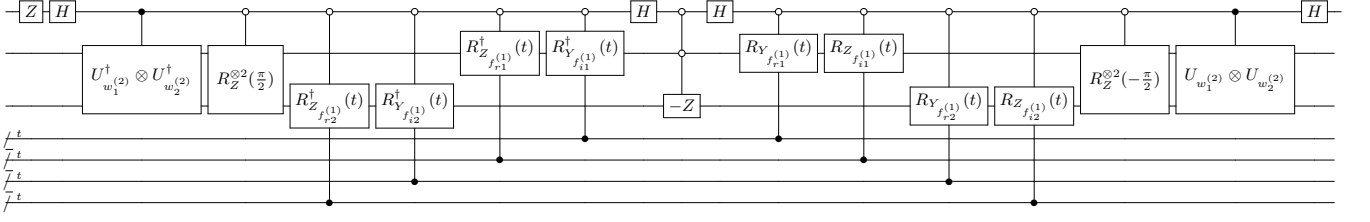


FIG. 11. The transformation $G_{r1}^{(2)}$.

$\theta_i \in \{\beta_{ijk}, \gamma_{ijk}, \delta_{ijk}\}$ and $L = |\{\beta_{ijk}, \gamma_{ijk}, \delta_{ijk}\}|$. As the Figure 8 and the Figure 10(b), the output state $|z^i\rangle$ always can be obtained by performing a unitary transformation, denoted by $U^i(\theta)$, to the initial state $|0\rangle$ and adding some measurements. Let $|Z^i\rangle = U^i(\theta)|0\rangle$, then the output state $|z^i\rangle$ is decided by the parameter vector θ and measurement results. Denote the map from $|0\rangle$ to $|z^i\rangle$ by $F^i(\theta)$. Thus, \mathcal{L} can be viewed as a function of θ .

We explain the training process as follows.

Step 1. Initial value selection. Randomly try the initial parameter vector θ and choose the optimal parameter denoted by $\theta^{(0)}$ such that the value of \mathcal{L} is minimum.

The value of $\text{Re}\langle z^i | d^i \rangle$ for each vector θ can be obtained by reusing quantum swap test. Then classically calculate and compare the different values of $\mathcal{L}(\theta)$ to obtain the optimal initial value.

Step 2. Iteration process. We use the gradient descent method. In the $(i+1)$ -th step,

$$\theta_l^{(i+1)} = \theta_l^{(i)} - \eta \frac{\partial \mathcal{L}}{\partial \theta_l}, \quad (19)$$

where η is an adjustable positive step length and $l = 1, \dots, L$. Combining the expressions (17)(19), we can use the quantum-classical hybrid method to acquire the gradient.

$$\frac{\partial \mathcal{L}}{\partial \theta_l} = -\frac{2}{q} \sum_{i=1}^q \frac{\text{Re} \partial \langle d^i | z^i \rangle}{\partial \theta_l}, \quad (20)$$

$$\frac{\partial |z^i\rangle}{\partial \theta_l} = \frac{\partial F^i}{\partial \theta_l} |0\rangle. \quad (21)$$

The partial derivative of F^i can be obtained by firstly deriving the partial derivative of U^k and then add the corresponding measurements.

To be specific, theoretically for arbitrary unitary transformation, it always can be represented by the basic unitary gates: the single particle rotation gates and the control X gates. For example, if $U^i = (R_X(2g_1(\theta_l)) \otimes R_Z(2g_2(\theta_l)))(CNOT)(I \otimes R_Z(2g_3(\theta_l)))$, where $g_j(\theta_l) \in [0, 2\pi)$ denotes the rotation angle for the single particle gate in the form by the basic unitary gates, $j = 1, 2, 3$.

$$\frac{\partial U^i |0\rangle}{\partial \theta_l} = -g'_1(\theta_l) |i(X \otimes I)U^i|0\rangle - g'_2(\theta_l) |i(I \otimes Z)U^i|0\rangle. \quad (22)$$

As expression (22), we can construct the quantum circuit for the unitary transformation $i(X \otimes I)U^i$ and $i(I \otimes Z)U^i$,

respectively. Then measure and record the corresponding registers, collapsing $i(X \otimes I)U^i|0\rangle$ and $i(I \otimes Z)U^i|0\rangle$ to the states denoted by $|z_{p1}^i\rangle$ and $|z_{p2}^i\rangle$, respectively. At last, we use swap test to get the value of $\text{Re}\langle d^i | z_{p1}^i \rangle$ and $\text{Re}\langle d^i | z_{p2}^i \rangle$ and calculate the gradient of \mathcal{L} by

$$\frac{\text{Re} \partial \langle d^i | z^i \rangle}{\partial \theta_l} = -g'_1(\theta_l) \text{Re}\langle d^i | z_{p1}^i \rangle - g'_2(\theta_l) \text{Re}\langle d^i | z_{p2}^i \rangle.$$

VI. NUMERICAL EXPERIMENT: CLASSIFICATION ON A CHECKERBOARD

In this section, we numerically validate our model with the following checkerboard classification task.

Consider a product state $R_Y(\theta_1)|0\rangle \otimes R_Y(\theta_2)|0\rangle$. This state has two parameters $\theta_1, \theta_2 \in [0, 2\pi)$, which forms a square area $C \triangleq \{[0, 2\pi) \times [0, 2\pi)\}$. Now, suppose we divide the square C into a 2×2 checkerboard with two disjoint parts:

$$\begin{aligned} C_0 &= \{[0, \pi) \times [0, \pi)\} \cup \{[\pi, 2\pi) \times [\pi, 2\pi)\} \\ C_1 &= \{[0, \pi) \times [\pi, 2\pi)\} \cup \{[\pi, 2\pi) \times [0, \pi)\} \end{aligned} \quad (23)$$

The task is to classify whether the input quantum state is in the region C_0 (labeled by $|0\rangle$) or C_1 (labeled by $|1\rangle$). To this end, we constructed a 4-layered quantum neural network: the input layer has two neurons corresponding to the input state, followed by two hidden layers with 8 neurons in each of them, and the output layer has one neuron.

During the training process, we randomly generated 10^5 data points, and applied the stochastic gradient descent algorithm to minimize the loss function defined in equation (17). In this numerical experiment, since the vector forms of samples are known, we calculated the loss function and the gradient in the classical way. The learning curve is shown in Figure 12, from which we can see that the loss converged to about 0.23.

After training, we further generated 10,000 samples to test our quantum neural network. The result is plotted in Figure 13, in which the classification accuracy achieved 99.25%.

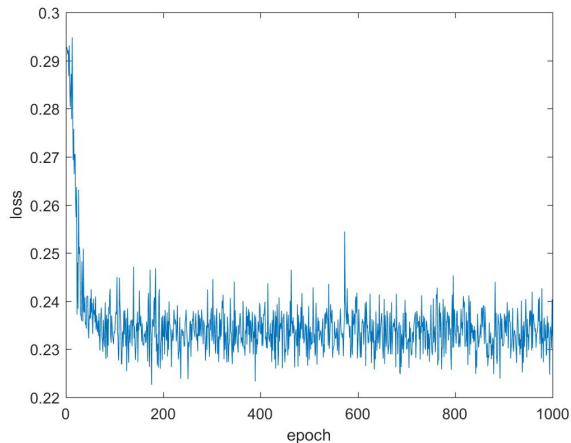


FIG. 12. The learning curve

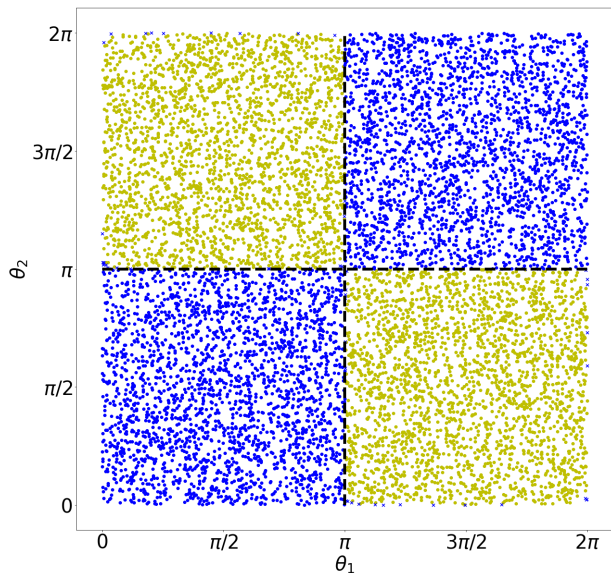


FIG. 13. The testing result: The correct predictions are represented with dots, and the incorrect predictions are labeled with crosses.

VII. CONCLUSIONS

The quantum neural network is introduced and its explicit expression is obtained. The validity of the training process of neural network is proved theoretically. The numerical example illustrates the potential of this model. Although there exists the process of measurement, we do not need to record or store any measured result, which means performing the quantum neural networks do not cost the resources for classical calculations.

This proposed quantum neural network includes some situations of classical neural network, where the weights constitute a vector belonging to the product state space. And it can be used to process both quantum data with classical labels directly and classical data with classical

labels by using state preparation.

A possible future research topic is to generalize the form of the weights in each layer, such as $|w_j^{(k)}\rangle$ is not limited to the product state. One can also generalize the activation operator f , which still retains the validity or to generalize output state of neural network into a entangled state.

ACKNOWLEDGEMENTS

This work was supported by the National Key Research and Development Program of China (Grant No. 2016YFA0301700) and the Anhui Initiative in Quantum Information Technologies (Grant No. AHY080000).

APPENDIX

A. THE PROOF OF THEOREM 1

Proof. Denote $y'_r = \lfloor 2^t \theta_r / \pi \rfloor$ and $y''_r = 2^t - y'_r$ (see equation (4) for the meaning of θ_r). By quantum phase estimation (see [31]), $\forall \sigma' \in (0, 1)$ we can choose $t = m + \lceil \log_2(2 + \frac{1}{2\sigma'}) \rceil$ and approximate θ_r / π to precision 2^{-m} with probability at least $1 - \sigma'$, thus the exact form of the state $|\psi_r\rangle$ in equation (8) should be

$$\begin{aligned} & \frac{-i}{\sqrt{2}} \left[e^{i\theta} \left(\sum_{\substack{\tilde{y}'_r: |\tilde{y}'_r - y'_r| \\ \leq 2^{t-m-1}}} \beta_{\tilde{y}'_r} |\tilde{y}'_r\rangle + \sum_{\substack{\tilde{y}''_r: |\tilde{y}''_r - y''_r| \\ > 2^{t-m-1}}} \beta_{\tilde{y}''_r} |\tilde{y}''_r\rangle \right) |w_+\rangle \right. \\ & \left. - e^{-i\theta} \left(\sum_{\substack{\tilde{y}''_r: |\tilde{y}''_r - y''_r| \\ \leq 2^{t-m-1}}} \beta_{\tilde{y}''_r} |\tilde{y}''_r\rangle + \sum_{\substack{\tilde{y}'_r: |\tilde{y}'_r - y'_r| \\ > 2^{t-m-1}}} \beta_{\tilde{y}'_r} |\tilde{y}'_r\rangle \right) |w_-\rangle \right]. \end{aligned} \quad (\text{A1})$$

Moreover,

$$\sum_{\substack{\tilde{y}'_r: |\tilde{y}'_r - y'_r| \\ \leq 2^{t-m-1}}} \frac{|\beta_{\tilde{y}'_r}|^2}{2} \geq \frac{1 - \sigma'}{2}, \quad \sum_{\substack{\tilde{y}''_r: |\tilde{y}''_r - y''_r| \\ \leq 2^{t-m-1}}} \frac{|\beta_{\tilde{y}''_r}|^2}{2} \geq \frac{1 - \sigma'}{2}.$$

In $|\psi_r\rangle$, all \tilde{y}'_r provide 2^{-m} approximates of θ_r / π , i.e., $|\tilde{y}'_r / 2^t - \theta_r / \pi| \leq 2^{-m}$. We also have $\tilde{y}''_r = 2^t - \tilde{y}'_r$. Apply control rotation shown in Figure 6(a) to $|\psi_r\rangle|0\rangle$, then with probability at least $1 - \sigma'$, we get

$$|\tilde{d}'_r\rangle = R_Y(\tilde{y}'_r \pi / 2^{t-1})|0\rangle \quad (\text{A2})$$

in the third register. Denote the the angle between $|\tilde{d}'_r\rangle$ and $|d_r\rangle := R_Y(2\theta_r)|0\rangle$ in Bloch sphere as η_r , then

$$\eta_r = \left| \tilde{y}'_r - \frac{2^t \theta_r}{\pi} \right| \frac{\pi}{2^{t-1}} \leq \frac{\pi}{2^{m-1}}. \quad (\text{A3})$$

Thus,

$$\| |\tilde{d}'_r\rangle - |d_r\rangle \| \leq \sqrt{2 - 2 \cos(\eta_r / 2)} = 2 \sin(\eta_r / 4) \leq \pi / 2^m. \quad (\text{A4})$$

Similarly, with probability at least $1 - \sigma'$, we can obtain a \tilde{y}''_r such that $|\tilde{y}''_r / 2^t - \theta_r / \pi| \leq 2^{-m}$. By definition,

$$\begin{aligned} |\tilde{d}\rangle &= R_Z(-\pi/2) R_Z(\tilde{y}''_r \pi / 2^{t-1}) R_Y(\tilde{y}''_r \pi / 2^{t-1}) |0\rangle, \\ |d\rangle &= R_Z(-\pi/2) R_Z(2\theta_i) R_Y(2\theta_r) |0\rangle. \end{aligned}$$

Therefore,

$$\begin{aligned} & \| |\tilde{d}\rangle - |d\rangle \| \\ & \leq \| R_Z(\tilde{y}''_r \pi / 2^{t-1}) (R_Y(\tilde{y}''_r \pi / 2^{t-1}) |0\rangle \\ & \quad - R_Z(\tilde{y}''_r \pi / 2^{t-1}) R_Y(2\theta_r) |0\rangle) \| \\ & \quad + \| R_Z(\tilde{y}''_r \pi / 2^{t-1}) R_Y(2\theta_r) |0\rangle \\ & \quad - R_Z(2\theta_i) R_Y(2\theta_r) |0\rangle \| \\ & \leq \| |\tilde{d}'_r\rangle - |d_r\rangle \| + \| R_Z(\tilde{y}''_r \pi / 2^{t-1}) - R_Z(2\theta_i) \| \\ & \leq \pi / 2^m + \pi / 2^m = \pi / 2^{m-1}. \end{aligned}$$

The success probability is $(1 - \sigma')^2 > 1 - 2\sigma'$. We choose $\sigma = 2\sigma' \in (0, 1)$ and $t = m + \lceil \log_2(2 + \frac{1}{\sigma}) \rceil$. ■

B. THE DETAILS OF THEOREM 2

Lemma 1. Assume that $|x\rangle = |x_1, \dots, x_n\rangle, |\tilde{x}\rangle = |\tilde{x}_1, \dots, \tilde{x}_n\rangle$, where $\| |x_i\rangle - |\tilde{x}_i\rangle \| \leq \epsilon$ for all i . Assume that $|w\rangle = |w_1, \dots, w_n\rangle$. Then

- (1). $\| |x\rangle - |\tilde{x}\rangle \| \leq n\epsilon$.
- (2). Let $g(y) = \arccos(-y)$, $y \in [-1, 1]$. $\forall \delta \in (0, 2)$, if $|y_1 - y_2| < \delta$, then

$$|g(y_1) - g(y_2)| \leq \pi \sqrt{\delta} / \sqrt{2}.$$

- (3). Suppose that $y_r \pi / 2^{t-1}, y_i \pi / 2^{t-1}, \tilde{y}_r \pi / 2^{t-1}, \tilde{y}_i \pi / 2^{t-1}$ are $\pi / 2^m$ approximates of $2\theta_r = \arccos -\mathbf{Re}\langle x|w\rangle, 2\theta_i = \arccos -\mathbf{Im}\langle x|w\rangle, \arccos -\mathbf{Re}\langle \tilde{x}|w\rangle, \arccos -\mathbf{Im}\langle \tilde{x}|w\rangle$ respectively, then

$$|\tilde{d}\rangle = R_Z(-\pi/2) R_Z(\tilde{y}_i \pi / 2^{t-1}) R_Y(\tilde{y}_r \pi / 2^{t-1}) |0\rangle,$$

$$|d\rangle = R_Z(-\pi/2) R_Z(2\theta_i) R_Y(2\theta_r) |0\rangle,$$

satisfies $\| |\tilde{d}\rangle - |d\rangle \| \leq \pi / 2^{m-1} + \pi \sqrt{n\epsilon} / \sqrt{2}$.

Proof. (1). We prove the result by induction. The result is true for $n = 1$. Denote $|x'\rangle = |x_2, \dots, x_n\rangle$ and $|\tilde{x}'\rangle = |\tilde{x}_2, \dots, \tilde{x}_n\rangle$, then by induction $\| |x'\rangle - |\tilde{x}'\rangle \| \leq (n-1)\epsilon$. Thus

$$\begin{aligned} \| |x\rangle - |\tilde{x}\rangle \| & \leq \| |x_1, x'\rangle - |\tilde{x}_1, x'\rangle \| + \| |\tilde{x}_1, x'\rangle - |\tilde{x}_1, \tilde{x}'\rangle \| \\ & \leq n\epsilon. \end{aligned}$$

- (2). Since $|y_1 - y_2| \leq \delta$, we have $|g(y_1) - g(y_2)| \leq \arccos(1 - \delta)$. Note that $\cos(\pi \sqrt{\delta} / \sqrt{2}) < 1 - \delta$, then $|g(y_1) - g(y_2)| \leq \pi \sqrt{\delta} / \sqrt{2}$.

- (3). By (1), we have $\| |x\rangle - |\tilde{x}\rangle \| \leq n\epsilon$, thus $|\langle w|x\rangle - \langle w|\tilde{x}\rangle| \leq n\epsilon$. Denote $2\tilde{\theta}_r = \arccos -\mathbf{Re}\langle \tilde{x}|w\rangle, 2\tilde{\theta}_i = \arccos -\mathbf{Im}\langle \tilde{x}|w\rangle$, then by (2), $|\tilde{\theta}_r - \theta_r| \leq \pi \sqrt{n\epsilon} / 2\sqrt{2}, |\tilde{\theta}_i - \theta_i| \leq \pi \sqrt{n\epsilon} / 2\sqrt{2}$. Set $|d'\rangle = R_Z(-\pi/2) R_Z(2\tilde{\theta}_i) R_Y(2\tilde{\theta}_r) |0\rangle$, then

$$\begin{aligned} \| |\tilde{d}\rangle - |d\rangle \| & \leq \| |\tilde{d}\rangle - |d'\rangle \| + \| |d'\rangle - |d\rangle \| \\ & \leq \pi / 2^{m-1} + \pi \sqrt{n\epsilon} / \sqrt{2}. \end{aligned}$$

This completes the proof. ■

Then combining lemma 1 and theorem 1, we give the proof of theorem 2.

Proof. Denote the error to generate $|z^{(k)}\rangle$ as ϵ_k , then $\epsilon_0 = 0$. Assume that $m = \lceil \log_2(\pi / \delta) \rceil + 1$ for some δ such that $\delta \leq \frac{\pi}{\sqrt{2}} \sqrt{\epsilon_k}$ for all $k \geq 1$.

By lemma 1, $\epsilon_1 \leq p_1 \frac{\pi}{2^{m-1}} \leq p\delta$. When $k \geq 2$ and $\epsilon_{k-1} \leq 2$,

$$\begin{aligned} \epsilon_k & \leq p_k \left(\frac{\pi}{2^{m-1}} + \frac{\pi}{\sqrt{2}} \sqrt{\epsilon_{k-1}} \right) \\ & \leq p(\delta + \frac{\pi}{\sqrt{2}} \sqrt{\epsilon_{k-1}}) \\ & \leq \sqrt{2} p \sqrt{\epsilon_{k-1}}. \end{aligned}$$

Thus,

$$\begin{aligned}\epsilon_k &\leq (\sqrt{2\pi})^{1+\frac{1}{2}+\dots+\frac{1}{2^{k-2}}} p^{1+\frac{1}{2}+\dots+\frac{1}{2^{k-1}}} \delta^{\frac{1}{2^{k-1}}} \\ &\leq 2\pi^2 p^2 \delta^{\frac{1}{2^{k-1}}}.\end{aligned}$$

Setting $\epsilon_K = \epsilon$ shows that $\delta = (\epsilon/2\pi^2 p^2)^{2^{K-1}}$. And we

can check that $\epsilon_k < 2\pi^2 p^2 \delta^{\frac{1}{2^{k-1}}} < \epsilon < 2$.

By theorem 1, if $t = m + \log_2(2 + \frac{1}{\sigma'})$ the success probability is $(1 - \sigma')^{Kp}$. Let $\sigma = Kp\sigma' \in (0, 1)$, then

$$(1 - \sigma')^{Kp} = (1 - \frac{\sigma}{Kp})^{Kp} \geq 1 - \sigma.$$

■

-
- [1] Warren S McCulloch and Walter Pitts. A logical calculus of the ideas immanent in nervous activity. *The bulletin of mathematical biophysics*, 5(4):115–133, 1943.
- [2] Frank Rosenblatt. *The perceptron, a perceiving and recognizing automaton Project Para*. Cornell Aeronautical Laboratory, 1957.
- [3] Marvin Minsky and Seymour A Papert. *Perceptrons: An introduction to computational geometry*. MIT press, 2017.
- [4] J Hospfield. Neural networks and physical systems with emergent collective computer abilities. *Proc Natl Acad Sci*, 79(6):2554–2558, 1982.
- [5] Imad A Basheer and Maha Hajmeer. Artificial neural networks: fundamentals, computing, design, and application. *Journal of microbiological methods*, 43(1):3–31, 2000.
- [6] Henrique Steinherz Hippert, Carlos Eduardo Pedreira, and Reinaldo Castro Souza. Neural networks for short-term load forecasting: A review and evaluation. *IEEE Transactions on power systems*, 16(1):44–55, 2001.
- [7] Subhash Kak. On quantum neural computing. *Information Sciences*, 83(3-4):143–160, 1995.
- [8] Maria Schuld, Ilya Sinayskiy, and Francesco Petruccione. The quest for a quantum neural network. *Quantum Information Processing*, 13(11):2567–2586, 2014.
- [9] MV Altaisky. Quantum neural network. *arXiv preprint quant-ph/0107012*, 2001.
- [10] M Andreucut and MK Ali. A quantum neural network model. *International Journal of Modern Physics C*, 13(01):75–88, 2002.
- [11] Adenilton José da Silva, Teresa Bernarda Ludermir, and Wilson Rosa de Oliveira. Quantum perceptron over a field and neural network architecture selection in a quantum computer. *Neural Networks*, 76:55–64, 2016.
- [12] Kwok Ho Wan, Oscar Dahlsten, Hlér Kristjánsson, Robert Gardner, and MS Kim. Quantum generalisation of feedforward neural networks. *npj Quantum Information*, 3(1):36, 2017.
- [13] Yudong Cao, Gian Giacomo Guerreschi, and Alán Aspuru-Guzik. Quantum neuron: an elementary building block for machine learning on quantum computers. *arXiv preprint arXiv:1711.11240*, 2017.
- [14] Edward Farhi and Hartmut Neven. Classification with quantum neural networks on near term processors. *arXiv preprint arXiv:1802.06002*, 2018.
- [15] Ammar Daskin. A simple quantum neural net with a periodic activation function. *arXiv preprint arXiv:1804.07633*, 2018.
- [16] Géza Tóth, Craig S Lent, P Douglas Tougaw, Yuriy Brazhnik, Weiwen Weng, Wolfgang Porod, Ruey-Wen Liu, and Yih-Fang Huang. Quantum cellular neural networks. *Superlattices and Microstructures*, 20(4):473–478, 1996.
- [17] Changpeng Shao. A quantum model for multilayer perceptron. *arXiv preprint arXiv:1808.10561*, 2018.
- [18] Alexander I Lvovsky and Michael G Raymer. Continuous-variable optical quantum-state tomography. *Reviews of Modern Physics*, 81(1):299, 2009.
- [19] Andrei N Soklakov and Rüdiger Schack. State preparation based on grovers algorithm in the presence of global information about the state. *Optics and spectroscopy*, 99(2):211–217, 2005.
- [20] Andrei N Soklakov and Rüdiger Schack. Efficient state preparation for a register of quantum bits. *Physical Review A*, 73(1):012307, 2006.
- [21] Francesco Tacchino, Chiara Macchiavello, Dario Gerace, and Daniele Bajoni. An artificial neuron implemented on an actual quantum processor. *arXiv preprint arXiv:1811.02266*, 2018.
- [22] Seth Lloyd, Masoud Mohseni, and Patrick Rebentrost. Quantum algorithms for supervised and unsupervised machine learning. *arXiv preprint arXiv:1307.0411*, 2013.
- [23] Seth Lloyd, Masoud Mohseni, and Patrick Rebentrost. Quantum principal component analysis. *Nature Physics*, 10(9):631, 2014.
- [24] Xin-Ding Zhang, Xiao-Ming Zhang, and Zheng-Yuan Xue. Quantum hyperparallel algorithm for matrix multiplication. *Scientific reports*, 6:24910, 2016.
- [25] Terence D Sanger. Optimal unsupervised learning in a single-layer linear feedforward neural network. *Neural networks*, 2(6):459–473, 1989.
- [26] George Bebis and Michael Georgiopoulos. Feed-forward neural networks. *IEEE Potentials*, 13(4):27–31, 1994.
- [27] Guang-Bin Huang, Qin-Yu Zhu, and Chee-Kheong Siew. Extreme learning machine: a new learning scheme of feedforward neural networks. In *Neural Networks, 2004. Proceedings. 2004 IEEE International Joint Conference on*, volume 2, pages 985–990. IEEE, 2004.
- [28] Alberto Peruzzo, Jarrod McClean, Peter Shadbolt, Man-Hong Yung, Xiao-Qi Zhou, Peter J Love, Alán Aspuru-Guzik, and Jeremy L O'Brien. A variational eigenvalue solver on a photonic quantum processor. *Nature communications*, 5:4213, 2014.
- [29] Edward Farhi, Jeffrey Goldstone, and Sam Gutmann. A quantum approximate optimization algorithm. *arXiv preprint arXiv:1411.4028*, 2014.
- [30] Kosuke Mitarai, Makoto Negoro, Masahiro Kitagawa, and Keisuke Fujii. Quantum circuit learning. *Physical Review A*, 98(3):032309, 2018.
- [31] Michael A Nielsen and Isaac Chuang. Quantum computation and quantum information, 2002.